Proceedings of the ASME 2015 International Technical Conference and Exhibition on Packaging and Integration of Electronic and Photonic Microsystems and ASME 2015 12th International Conference on Nanochannels, Microchannels, and Minichannels
InterPACKICNMM2015
July 6-9, 2015, San Francisco, California, USA

InterPACKICNMM2015-48423

THE EFFECTIVENESS OF DATA CENTER OVERHEAD COOLING IN STEADY AND TRANSIENT SCENARIOS: COMPARISON OF DOWNWARD FLOW TO A COLD AISLE VERSUS UPWARD FLOW FROM A HOT AISLE

Luis Silva-Llanca*
Departamento de Ingeniería Mecánica
Universidad de La Serena
La Serena, Chile

Marcelo del Valle
Alfonso Ortega
Laboratory for Advanced Thermal and Fluid Systems
Department of Mechanical Engineering
Villanova University
Villanova, Pennsylvania, 19085

ABSTRACT

The most common approach to air cooling of data centers involves the pressurization of the plenum beneath the raised floor and delivery of air flow to racks via perforated floor tiles. This cooling approach is thermodynamically inefficient due in large part to the pressure losses through the tiles. Furthermore, it is difficult to control flow at the aisle and rack level since the flow source is centralized rather than distributed. Distributed cooling systems are more closely coupled to the heat generating racks. In overhead cooling systems, one can distribute flow to distinct aisles by placing the air mover and water cooled heat exchanger directly above an aisle. Two arrangements are possible: (i.) placing the air mover and heat exchanger above the cold aisle and forcing downward flow of cooled air into the cold aisle (Overhead Downward Flow (ODF)), or (ii.) placing the air mover and heat exchanger above the hot aisle and forcing heated air upwards from the hot aisle through the water cooled heat exchanger (Overhead Upward Flow (OUF)). This study focuses on the steady and transient behavior of overhead cooling systems in both ODF and OUF configurations and compares their cooling effectiveness and energy efficiency. The flow and heat transfer inside the servers and heat exchangers are modeled using physics based approaches that result in differential equation based mathematical descriptions. These models are programmed in the MATLAB™ language and embedded within a CFD computational environment (using the commercial code FLUENT™) that computes the steady or instantaneous airflow distribution. The complete computational model is able to simulate the complete flow and thermal field in the airside, the instantaneous temperatures within and pressure drops through the servers, and the instantaneous temperatures within and pressure drops through the overhead cooling system. Instantaneous overall energy consumption (1st Law) and exergy destruction (2nd Law) were used to quantify overall energy efficiency and to identify inefficiencies within the two systems. The server cooling effectiveness, based on an effectiveness-NTU model for the servers, was used to assess the cooling effectiveness of the two overhead cooling approaches.

INTRODUCTION

Scarce academic work on overhead cooling systems can be found in the literature. The majority of the information available is provided by the equipment suppliers in catalogs and manuals. Within the few publications about the topic, the overhead modules are utilized as a secondary cooling source. Heydari

*Address all correspondence to this author; lsilva@userena.cl

and Sabounchi [1] and Heydari [2], used CFD simulations to model overhead cooling systems in combination with CRAH units. Heat exchanger analytical models were integrated into the CFD software used. The studies showed that overhead cooling systems are effective in the presence of hot spots when they are used as an additional cold air supplier, especially in high power density cases. Other authors [3] have used CFD simulations to compare overhead systems with different cooling technologies. It was concluded that overheads can prevent recirculation at the top of the cabinets when they are use in open configurations. For the cabinets near the top of the rack, an inadequate provision of air was observed due the high momentum in the cold air jet leaving the overhead. The CFD data indicated that overhead systems had can handle high power rack densities, although they presented difficulties in building enough static pressure in low power densities.

In the current work, we use computational fluid dynamics to perform a detailed examination of the fluid flow in overhead cooling scenarios not only to investigate the cooling effectiveness but also to examine the energy efficiency of that cooling approach. Energy efficiency can be examined by locating the inefficiencies in the cooling system, and this is best done by mapping the Entropy generation, or equivalently, the Exergy destruction, within the system. This approach is not new but has found increasing acceptance in examination of data center thermal management schemes. In data centers the technique was first introduced by Shah and co-investigators [Shah reference here]. Entropy generation, or exergy destruction, have been examined in both laminar and turbulent flows [4–6]. Kock and Herwig [4, 6], developed a formulation to study turbulent flows from a second law perspective, and demonstrated how turbulent fluctuations enhance irrevesibilities. Herwig [7] presented an overview of the state of the art in turbulent flows that is highly applicable to data center air flows.

Silva-Llanca et al. [8] compared two numerical models for the calculation of exergy destruction in perimeter cooled data center turbulent flows using data obtained from CFD simulation. The first method was derived from the direct application of the second law inside a given grid control volume (direct method), whereas the second was based on Kock and Herwig [4] (indirect method). It was found that the entropy generation due to viscous dissipation (usually neglected in most applications), was approximately 36% of the total in the airspace, the pressure drop in the raised floor being the main contributor. The entropy generation due to heat conduction was attributed to the pre-mixing of cold and hot air streams in the cold aisle.

MOTIVATION AND GOALS

This study is motivated by two main gaps in our knowledge of how best to apply overhead systems: (1.) In application of overhead cooling, currently insufficient information exists to determine whether downward cold flow into a cold aisle (ODF) or upward heated flow (OUF) from a hot aisle is most effective and energy efficient, and (2.) in the use of distributed cooling systems such as overhead cooling, one of the potential future applications is in Dynamic On-Demand Cooling, wherein server work allocation and cooling are controlled synergistically such that cooling is provided only where and when needed.

The present study focuses on transient aspects of overhead cooling. Most notably, this study examines the transient behavior of such a system that includes the dynamic response of the cooling system heat exchangers, the servers, and the air flow. It will be shown that all three are important in establishing the dynamic response of the system.

This paper will discuss the first phase of an ambitious project aimed at developing performance metrics for energy optimized dynamically operated overhead cooling systems. The main goal of this first phase was to develop a transient numerical model that incorporated the effects of both servers and heat exchangers coupled with the transient air flow modeling. The use of that numerical model is demonstrated in this paper on a benchmark data center geometry that, although idealized, has allowed the development of the tools necessary to apply both first and second law thermodynamic principles in assessing the cooling effectiveness and energy efficiency of a generic system.

MATHEMATICAL MODEL AND NUMERICAL IMPLEMENTATION

The two cases studied in this work are shown schemtically in Fig. 1 (a) for the Overhead Downward Flow (ODF) or cold-aisle approach and (b) for the Overhead Upward Flow (OUF) or hot-aisle approach. The simulated room has 10 4U racks with 10 servers each and five ceiling mounted heat exchangers. A detailed depiction of the geometry is shown in Fig. 2. The transient behavior of the room is subject to the following assumptions:

- The room is isolated from the exterior (adiabatic walls)
- The aisle is fully contained, in other words, no leakage is allowed to or from the aisle
- Heat conduction exists between the aisle and the rest of the room
- The flow is assumed to be in turbulent regime
- Each server dissipates 1 kW throughout the process, for a total of 100 kW of required overhead cooling

Server transient model

The servers are modeled using the lumped approach demonstrated by Erden et al. [9] and Demetriou et al. [10] who treated the server as a black box, using a lumped capacitance model with

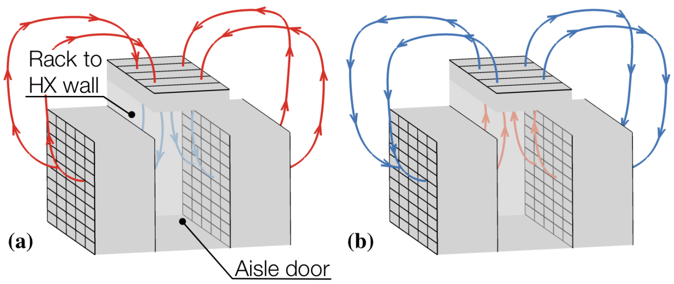

Figure 1: Schematic of the room for the two approaches: (a) downward flow, (b) upward flow.

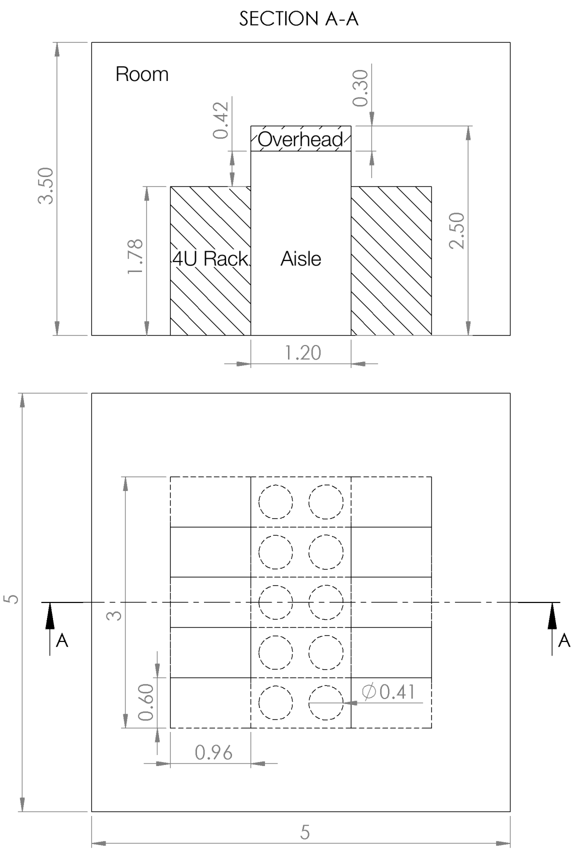

Figure 2: Two dimensional drawing for the data center room (dimensions in meters).

a constant air flow rate and no internal heat generation:

$$\theta(t) = \theta(0)e^{-t/\tau} \tag{1}$$

$$\theta = \frac{\dot{Q}_s}{K} - T_s + T_{s,in} \tag{2}$$

The server heat transfer is modeled using a heat exchanger approach wherein the server heated surface is assigned an average temperature Ts thereby allowing the introduction of a heat exchanger effectiveness which is a function of the Number of Transfer Units (NTU). The key to this approach is that the server thermal resistance, K, can be defined in terms of the server heat exchange effectiveness, ξ_s, and flow capacity, $\dot{C}_a$, as follows:

$$K = \xi_s \dot{C}_a \tag{3}$$

$$\xi_s = 1 - e^{-NTU} = f(\text{CFM}) \tag{4}$$

$$T_{s,in} - T_{s,out} = \xi_s (T_{s,in} - T_s) \tag{5}$$

The time constant τ and the effectiveness ξ_s for a 4U rack server were obtained as a function of the volumetric flow rate from [10].

Heat exchanger transient model

At the heart of any overhead cooling system is an air-to-liquid cross-flow heat exchanger. Because of the thermal mass of the heat exchanger materials and the coolant liquid, the dynamic thermal response of the heat exchanger depends on the heat exchanger materials and geometry, as well as the heat transfer properties of the coolant and its thermal mass. The transient behavior of cross flow heat exchangers has been widely studied since the 1950s. Because of the multi-dimensional and transient nature of the problem, no simple solution exists. A numerical and experimental study of a transient cross-flow heat exchanger was presented by del Valle and Ortega [11]. In their experiment, they introduced different temperature perturbations in the heat exchanger to analyze its transient response. The problem was numerically approximated using a finite difference approach, finding good to excellent agreement with the empirical data. The validated data was subsequently used to train an Artificial Neural Network (ANN) compact model. Compact models may be potentially used for predictions of the dynamic behavior of data centers with great accuracy, yet saving significant computational time when compared to CFD.

As demonstrated in [11], an energy balance in both streams and the wall provides a mathematical model to represent the cross flow heat exchanger transient behavior in the presence of time varying inlet air temperature or mass flow rate or inlet cooling temperature or mass flow rate. The result is a set three coupled partial differential equations.

The following assumptions and/or idealizations apply for this model: (i) Heat losses are negligible, (ii) there are no thermal energy sources or sink in the heat exchanger , (iii) there is no phase change in the fluids, (iv) the individual heat transfer coefficients are constant, and (v) wall thermal resistance is distributed uniformly in the entire heat exchanger and the axial heat conduction is negligible [12]. In order to generalize the results, the set of equations can be non-dimensionalized using the following set of parameters [13]:

$$\frac{\partial T_{wl}^*}{\partial t^*} + (1+R)T_{wl}^* = T_a^* + RT_w^* \tag{6}$$

$$V_a \frac{\partial T_a^*}{\partial t^*} + \frac{\partial T_a^*}{\partial x^*} + (T_a^* - T_{wl}^*) = 0 \tag{7}$$

$$V_w \frac{\partial T_w^*}{\partial t^*} + \frac{\partial T_w^*}{\partial x^*} + (T_w^* - T_{wl}^*) = 0 \tag{8}$$

Where:

$$x^* = \frac{(hA)_a x}{(\dot{m}c)_a L_a} \qquad y^* = \frac{(hA)_w y}{(\dot{m}c)_w L_w} \qquad T^* = \frac{T - T_{w,in}}{T_{a,in} - T_{w,in}} \tag{9}$$

$$t^* = \frac{(hA)_a}{(mc)_{wl}} \qquad V_w = \frac{(\dot{m}c)_w}{(mc)_{wl}} \frac{L_w}{u_w} \qquad V_a = \frac{(\dot{m}c)_a}{(mc)_{wl}} \frac{L_a}{u_a} \tag{10}$$

$$R = \frac{(hA)_w}{(hA)_a} \qquad NTU = \left\{ (\dot{m}c)_{\min} \left[\frac{1}{(hA)_a} + \frac{1}{(hA)_w} \right] \right\}^{-1} \tag{11}$$

The complete mathematical formulation may be found in [11].

Entropy generation

The rate of generation of entropy, or conversely, the destruction of exergy, is a measure of the rate at which irreversibilities occur in the data center systems. In the model geometry examined here, irreversibilities occur primarily in the heat exchanger due to pressure drop and heat exchange across finite temperature differences, in the server as a result of pressure drop and heat transfer from server heated surfaces to the air stream across a finite temperature difference, and finally in the air flow, primarily from thermal mixing and viscous dissipation.

The entropy generation in the servers and heat exchangers was derived in terms of inflows, outflows and storage terms as:

$$\left(\dot{S}'''_{gen,D'}\right)_s = \frac{ds}{dt} + \dot{m}c_p \ln\left(\frac{T_{s,out}}{T_{s,in}}\right) - \frac{\dot{Q}_s}{T_s} \tag{12}$$

$$\left(\dot{S}'''_{gen,D'}\right)_{HX} = \frac{ds}{dt} + \dot{m}c_p \ln\left(\frac{T_{HX,out}}{T_{HX,in}}\right) + \frac{\dot{Q}_{HX}}{T_w} \tag{13}$$

Bejan [14] developed a formulation for the local rate of entropy generation in convective heat transfer for an infinitesimal volume of fluid in laminar regime. This analysis was expanded to turbulent flows by Kock and Herwig [4] as follows:

$$\begin{aligned}
\dot{S}'''_{gen} = {} & \underbrace{\frac{\mu}{\overline{T}} \left\{ 2\left[\left(\frac{\partial \overline{v_x}}{\partial x}\right)^2 + \left(\frac{\partial \overline{v_y}}{\partial y}\right)^2 \right] + \left(\frac{\partial \overline{v_x}}{\partial y} + \frac{\partial \overline{v_y}}{\partial x} \right)^2 \right\}}_{\dot{S}'''_{gen,\overline{D}}} \\
& + \underbrace{\frac{\lambda}{\overline{T}^2} \left[\left(\frac{\partial \overline{T}}{\partial x}\right)^2 + \left(\frac{\partial \overline{T}}{\partial y}\right)^2 \right]}_{\dot{S}'''_{gen,\overline{C}}} \\
& + \underbrace{\frac{\mu}{\overline{T}} \left\{ 2\left[\overline{\left(\frac{\partial v'_x}{\partial x}\right)^2} + \overline{\left(\frac{\partial v'_y}{\partial y}\right)^2} \right] + \overline{\left(\frac{\partial v'_x}{\partial y} + \frac{\partial v'_y}{\partial x} \right)^2} \right\}}_{\dot{S}'''_{gen,D'}} \\
& + \underbrace{\frac{\lambda}{\overline{T}^2} \left[\overline{\left(\frac{\partial T'}{\partial x}\right)^2} + \overline{\left(\frac{\partial T'}{\partial y}\right)^2} \right]}_{\dot{S}'''_{gen,C'}}
\end{aligned} \tag{14}$$

The four terms in (14) are individualized as:

1. $\dot{S}'''_{gen,\overline{D}}$: entropy generation by direct dissipation.
2. $\dot{S}'''_{gen,D'}$: entropy generation by turbulent dissipation.
3. $\dot{S}'''_{gen,\overline{C}}$: entropy generation by heat conduction.
4. $\dot{S}'''_{gen,C'}$: entropy generation by heat transfer with fluctuating temperature gradients.

When used in conjunction with the k-ε model, $\dot{S}'''_{gen,D'}$ and $\dot{S}'''_{gen,C'}$ can be re-written as [4]:

$$\dot{S}'''_{gen,D'} = \frac{\rho \varepsilon}{\overline{T}} \tag{15}$$

$$\dot{S}'''_{gen,C'} = \frac{\alpha_t}{\alpha} \frac{\lambda}{\overline{T}^2} \left[\left(\frac{\partial \overline{T}}{\partial x}\right)^2 + \left(\frac{\partial \overline{T}}{\partial y}\right)^2 \right] \tag{16}$$

For more details about the derivation and the complete three-dimensional form, the reader may refer to [4].

Numerical procedure

The heat transfer and fluid dynamics inside the server and heat exchangers (Eqns. (1) to (13)) was solved using programming language software (MATLAB$^{\text{TM}}$). The unsteady turbulent convective heat transfer in the airside (aisle + room + Eq. (14)) was simulated via CFD software (ANSYS FLUENT$^{\text{TM}}$). As in most data center literature, the standard k-ε model was chosen to represent the turbulent flow. The air in the servers and heat exchangers was treated as ideal gas. The impedance and fan curves were assumed to be a quadratic function of the mass flow rate, resulting in server volumetric flow rates on the order of 50 CFM. To improve the numerical convergence in the early part of the process, the server flow was accelerated by weighing $\dot{m}_s$ with an s-shaped function ranging from zero to one during the first five seconds of physical time.

Table 1: Total entropy generation (W/K) for racks and airside (room-aisle) for each grid size tested.

	N of nodes	$\dot{S}_{gen}$ Servers	$\dot{S}_{gen}$ Airside
Mesh 1	108,573	203.5	0.059
Mesh 2	167,493	203.4	0.062
Mesh 3	315,671	203.3	0.073
Mesh 4	563,859	203.9	0.075

As described in the previous section, the simulation of servers and heat exchangers requires the simultaneous solution of a system of algebraic and ordinary differential equations. Commonly, commercially available CFD software, such as ANSYS FLUENT^{TM}, can only handle algebraic equations; therefore the necessity for a tool like MATLAB^{TM}.

The code proceeded as follows:

1. FLUENT iterates for one time step
2. The CFD data are used as inputs by MATLAB
3. MATLAB solves servers and heat exchangers equations
4. MATLAB data are imported as input boundary conditions into FLUENT
5. Back to step one under these new conditions

The fluid flow is uncoupled from the heat transfer, meaning that the velocity has no temperature dependence. This would not be the case in buoyant flow (natural convection) or when the properties such as viscosity and density depend on the temperature. The advantage of this uncoupled behavior is that the Navier-Stokes equations plus k and ε (six equations in total) need to be solved only until the flow develops. In other words, when the velocity field no longer varies, the code can be set to solve only for the temperatures, which greatly saves on computational costs.

In the present work it was found, for both cases (ODF and OUF), that the flow developed around $t = 7$ s. During this period the time step was kept constant at $dt = 0.005$ s. For $t > 7$ s, the time step was modified from 0.1 to 1 s until the process reached steady state, approximately at $t \approx 3400$ s.

Mesh validation

In order to meet grid size independence, four mesh densities were compared. Table 1 details the total entropy generation at the end of the process, for the servers and the airside. It can be seen that Mesh 3 presented an insignificant variation when compared to the mesh with the higher number of nodes (Mesh 4).

Figure 3 shows the influence of grid size variation upon the server temperature evolution. It can be observed that the data

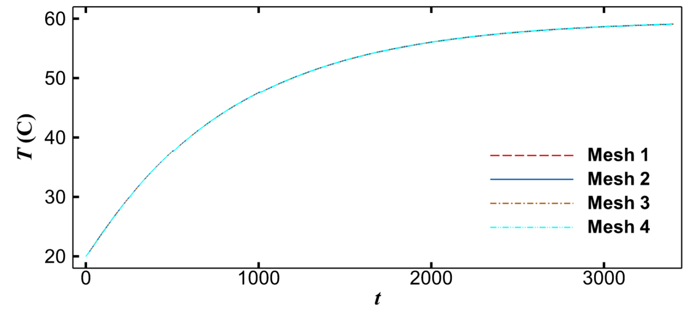

Figure 3: Mean temperature evolution in the servers vs time for different grid sizes.

demonstrated independence on the mesh density, since the four curves overlapped. Based on its sufficient accuracy, the third mesh size was chosen to carry the entirety of the simulations, as it completed the simulation faster than Mesh 4.

RESULTS AND DISCUSSION

Entropy generation in an idealized case

The temperature diagram in Fig. 4 represents the thermodynamic cycle for the overhead cooling process in steady state. If the entropy generation due to viscous dissipation (pressure drop) is neglected, and assuming ideal gas behavior, the second law states:

$$\dot{S}_{gen} = \dot{m}c_p \ln\left(\frac{T_{s,out}}{T_{s,in}}\right) + \dot{m}c_p \ln\left(\frac{T_{HX,out}}{T_{HX,in}}\right) - \frac{\dot{Q}_s}{T_s} + \frac{\dot{Q}_{HX}}{T_w} \tag{17}$$

The first two terms represent the entropy generation due to the heat transfer between aisle and room. The other two terms relate to the server heating and the overhead cooling. Equation (17) can be re-written in terms of inlet quantities and the server and heat exchanger thermal effectiveness:

$$N_S = \ln\left[\xi_s\left(\frac{T_s}{T_{s,in}-1}\right)+1\right] - \ln\left[\frac{T_w}{T_{HX,out}}\frac{1}{1-\xi_{HX}^{-1}} + \frac{1}{1-\xi_{HX}}\right] + \xi_s\left(1-\frac{T_{s,in}}{T_s}\right)\left(\frac{T_s}{T_w}-1\right) \tag{18}$$

Where $N_S \equiv \dot{S}_{gen}/\dot{m}c_p$ was defined by Bejan [14] as the entropy generation number.

Figure 5 shows N_S as a function of the effectiveness ratio ξ_s/ξ_{HX} for three different water to server temperature ratios. For fixed T_s/T_w, N_S was directly proportional to ξ_s/ξ_{HX}. This implies that the more effective is the heat transfer in the overhead, the lower is N_S. On the other hand, N_S increases with ξ_s/ξ_{HX}

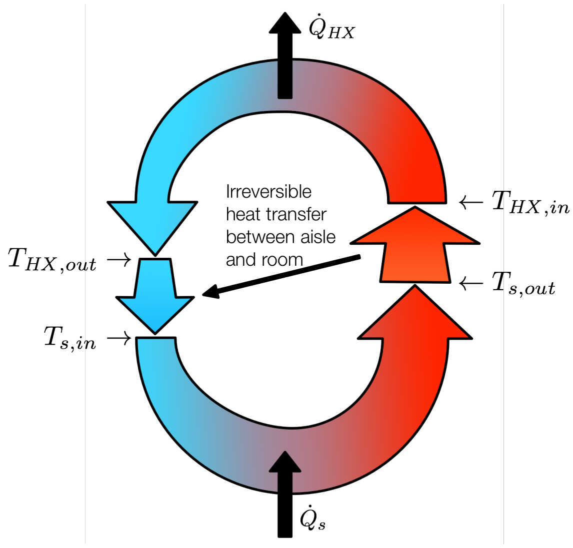

Figure 4: Temperature diagram for the heat exchange inside the room.

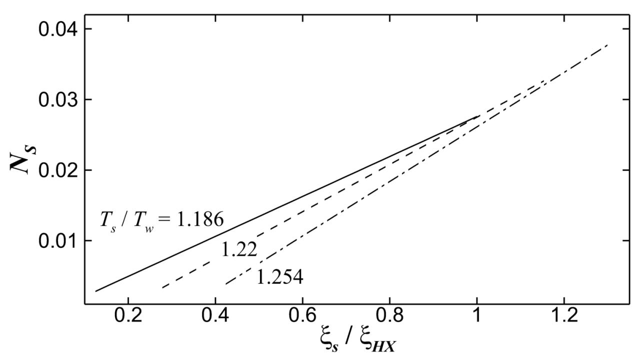

Figure 5: Entropy generation number as a function of the ratio ξ_s/ξ_{HX}.

as the servers transfer more heat to the cooling air stream. This is an example that illustrates that entropy generation minimization does not necessarily implies a zero $\dot{S}_{gen}$ goal. For instance, $\dot{S}_{gen} = 0$ means no heat transfer in the server, which opposes the objective of this thermal management study.

Steady state analysis

The temperature distribution for the two approaches is shown in Fig. 6. It can be seen that the temperature was relatively uniform in the aisle and room. Temperature gradients were found near the containment as these boundaries permitted heat flux through the boundary to the surrounding ambient.

The maximum possible heat transfer in the server can be achieved when the containment is insulated $\xi_{HX} = 1$ ($T_{HX,out} = T_w$), and when there is perfect heat transfer in the heat exchanger

Table 2: Mean value and standard deviation for the server and heat exchanger efficiency.

	ODF	OUF
$\bar{\eta}$	0.66	0.68
σ_η	0.0012	0.0006
$\bar{\xi}_{HX}$	0.83	0.86
$\sigma_{\xi_{HX}}$	0.031	0.0011

$\xi_s = 1$ ($T_{s,out} = T_s$):

$$\dot{Q}_{s,max} = \dot{m}c_p(T_s - T_w) \tag{19}$$

Using $\dot{Q}_{s,max}$, an overall cooling efficiency can be defined as:

$$\eta \equiv \frac{\dot{Q}_s}{\dot{Q}_{s,max}} = \frac{T_{s,out} - T_{s,in}}{T_s - T_w} \tag{20}$$

In Table 2 it can be seen that the OUF approach presented a slightly higher η. The standard deviation σ_η was 0.18% of $\bar{\eta}$ for ODF and 0.09% for OUF, demonstrating a fairly uniform distribution throughout the servers. The heat exchanger effectiveness ξ_{HX} was higher for OUF. Similarly to η, it showed a uniform distribution in the overheads.

The idealized analysis in the previous section showed that increasing ξ_{HX} (hypothetically up to 1) and increasing T_s, reduces the entropy generation. This also brings $\dot{Q}_s$ into its maximum possible value $\dot{Q}_{s,max}$; therefore from second law principles it is possible to arrive to the same optimum conditions utilized to define η in Eq. (20).

The entropy generation due to conduction $\dot{S}'''_{gen,C} = \dot{S}'''_{gen,\bar{C}} + \dot{S}'''_{gen,C'}$ and dissipation $\dot{S}'''_{gen,D} = \dot{S}'''_{gen,\bar{D}} + \dot{S}'''_{gen,D'}$ is shown in Fig. 7. In the case of $\dot{S}'''_{gen,C}$, the ODF approach presented the largest occupied volume. Two plumes can be observed for the OUF in the ZX view. They occurred because of the advection of $\dot{S}'''_{gen,C}$ provoked by the overhead fluid flowing upward the turning towards the servers. This generated a cold fluid vortex that acted as an insulator which reduced the heat flux through the rack-to-hx wall. This can be observed in Fig. 6 for the ZX views, where the temperature gradient near the rack-to-hx wall was narrower for OUF, leading to lower $\dot{S}'''_{gen,C}$.

For $\dot{S}'''_{gen,D}$, the OUF approach also presented the smallest values. Silva-Llanca et al. [8] demonstrated that large pressure drop in a legacy air-cooled data center accounted for the inefficiencies in the fluid flow, manifested in $\dot{S}'''_{gen,D}$. It can be seen

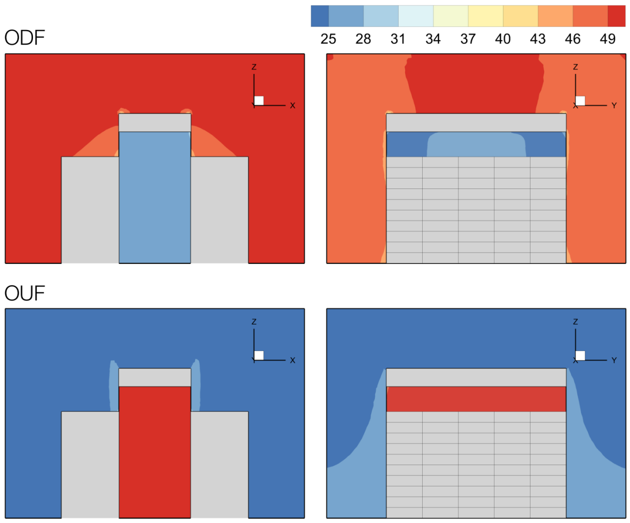

Figure 6: Temperature distribution inside the room for the two approaches.

Table 3: Total entropy generation (W/K) for racks, over-head heat exchangers and airside (room-aisle).

	Servers	Overheads	Airside
ODF	190.9	17.65	0.318
OUF	203.4	18.55	0.062

then, that the upward flow from the servers converging into the overheads generates less $\dot{S}'''_{gen,D}$ than a downward flow separating into multiple streams towards the servers.

Table 3 details the total $\dot{S}_{gen}$ for the servers, overheads and airside. The airside represented a small fraction of the entropy generation compared to the one in the cooling units, $\approx 1.78\%$. Interestingly, in studies of perimeter cooled data centers that did not utilize aisle containment, Silva-Llanca et al. [8] found this percentage to be $\approx 88\%$, whereas Shah et al. [15] estimated $\approx 50\%$. This demonstrates that containment greatly reduces inefficiencies in the airside at least for this highly idealized benchmark representation of a data center hot or cold aisle.

Unsteady behavior during the cooling process

As in the steady case, entropy is generated in the servers, heat exchanger, and in the air space during unsteady operation. During this process, the rate of entropy storage in each of these subsystems must be accounted for in the overall entropy budget. The rate of storage of entropy goes to zero as steady state is approached. The mean temperature evolution for the servers and overheads is shown in Figs. 8 and 9, respectively. It can be seen that T_s and T_{HX} grew exponentially, not affected by the early flow development ($t \leq 7$ s). Throughout the process, the ODF maintained lower server temperatures, even though $T_{HX,out}$ was higher and the efficiency η was similar in both approaches. This lower ODF T_s is consistent with the idealized analysis, where $\dot{S}_{gen}$ was lower for ODF in Table 3 as well. It is important to remark that the analysis of $\dot{S}_{gen}$ on the airside only might have led to erroneous conclusions, as this quantity becomes negligible compared to $\dot{S}_{gen}$ in the servers.

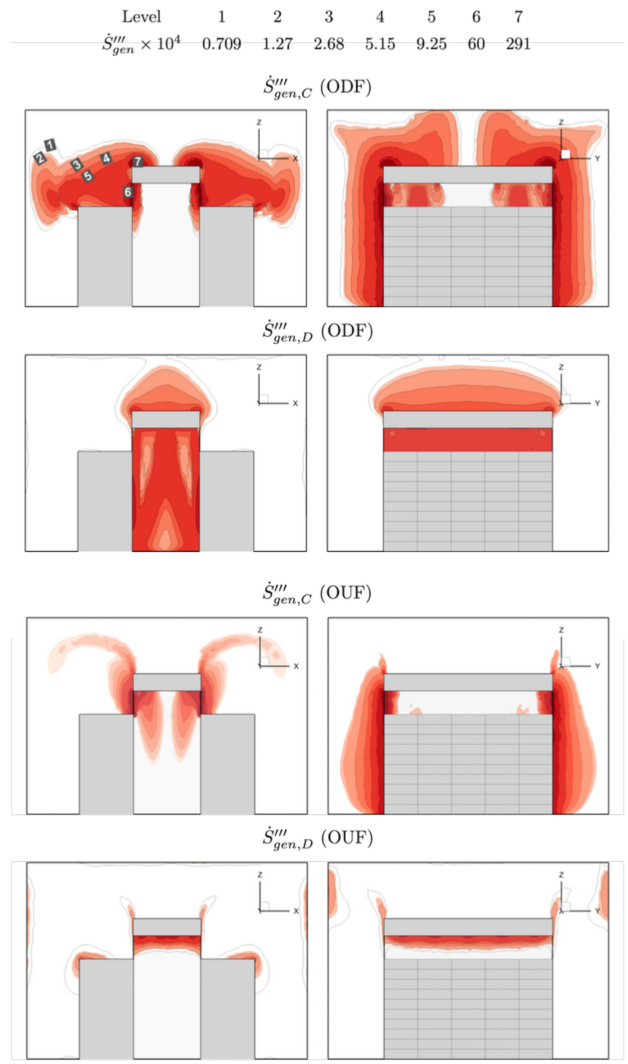

Figure 7: Conduction and dissipation entropy generation distribution inside the room for the two approaches.

Figure 8 also presents the evolution of the room mean efficiency $\bar{\eta}$. It can be observed that η remained relatively constant,

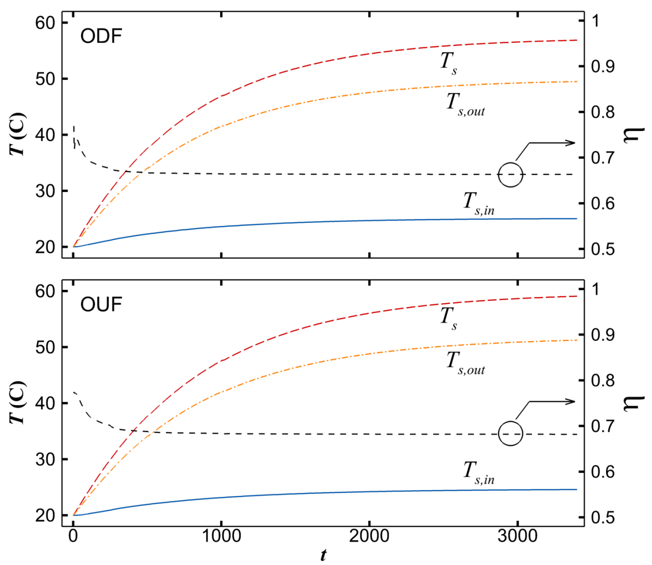

Figure 8: Mean temperature and mean efficiency evolution in the servers vs time.

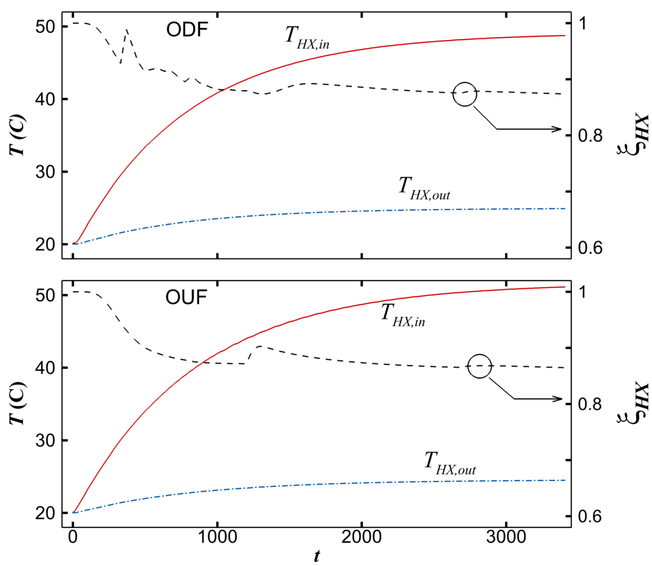

Figure 9: Mean temperature and mean efficiency in the overhead heat exchangers vs time.

especially after $t > 250$ s. This was not the same for the overhead effectiveness, which ranged from 1 to ≈ 0.8 (Fig. 9). A secondary peak was found at $t \approx 1600$ s for ODF and $t \approx 1300$ s for OUF. Although as of this point not conclusive, it can be speculated that this effect was related to the heat exchanger thermal mass.

The evolution of $\dot{S}'''_{gen}$ and its four components in the air-side is shown in Figs. 10 and 11 for the aisle and the room, respectively. Silva-Llanca et al. [8] demonstrated that the turbulent terms are the main contributors to $\dot{S}_{gen}$. This was observed in this problem for all the cases.

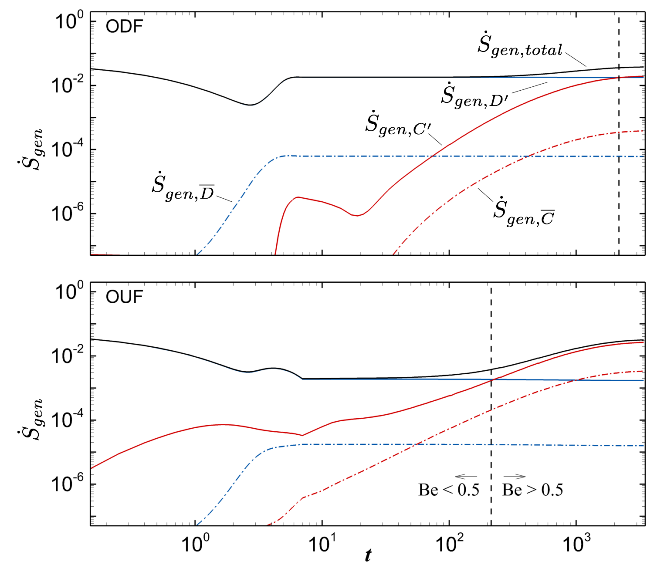

Figure 10: Entropy generation evolution inside the aisle.

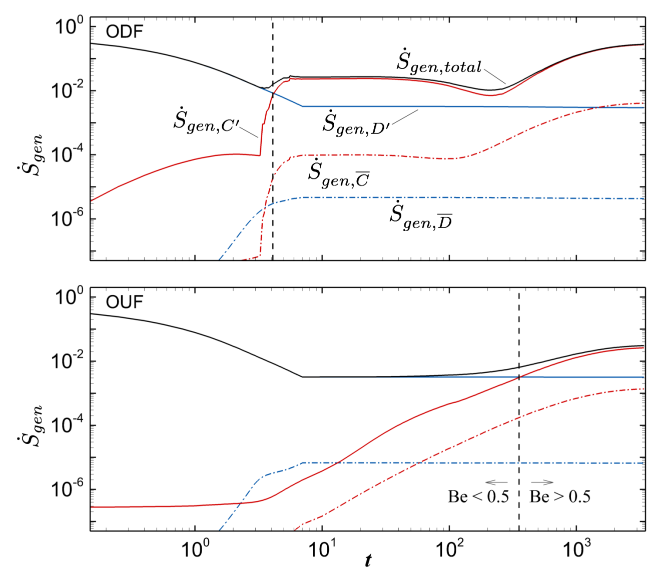

Figure 11: Entropy generation evolution in the room.

Entropy generation due to viscous dissipation (blue line) dominated during the early stages. As the temperatures started to increase, $\dot{S}_{gen,C}$ increased and surpassed $\dot{S}_{gen,D}$, becoming the main source of entropy generation.

Bejan [14] defined the irreversibility distribution ratio ϕ and the Bejan number as:

$$\phi \equiv \frac{\dot{S}'''_{gen}(\text{fluid friction})}{\dot{S}'''_{gen}(\text{heat transfer})} \tag{21}$$

$$\text{Be} \equiv (1+\phi)^{-1} \tag{22}$$

When $\dot{S}_{gen,D}$ dominates Be $\rightarrow 0$; when $\dot{S}_{gen,C}$ dominates Be $\rightarrow 1$. It can be seen in Figs. 10 and 11 that when Be $= 0.5$ (dashed line), $\dot{S}_{gen,D} = \dot{S}_{gen,C}$ as this coincided with the instant where the red and blue lines crossed.

CONCLUSIONS

A numerical code that simultaneously solves CFD and a system of algebraic and differential equations was developed to study the transient behavior of an overhead cooled data center with the effects of server and heat exchanger heat exchange effectiveness and thermal mass included, under two different scenarios. The main conclusions can be listed as follows:

1. The server temperature distribution was found to be fairly uniform. This was attributed to the distance allowed between the overheads and the racks that diminished the resistance when the flow was forced to turn into the servers. In the case of perimeter cooled data centers, perforated tile flow can present a detrimental effect on inlet flow uniformity in the racks.
2. A definition for an overall cooling efficiency was proposed using first law, ranging from zero to one for worst to best case scenario, respectively.
3. Based on a second law approach, and using a simplified analysis in an idealized case, optimum conditions are suggested. It was found that second law optimization led to the same conditions for cooling efficiency equals one.
4. The downward flow approach was the least efficient and generated the most entropy in the airside.
5. As expected, containment greatly decreased the entropy generation in the airside compared to prior work on uncontained perimeter cooled data centers.
6. The entropy generation in the servers far exceeded that in the heat exchangers and the room air flow. Because the containment caused the airflow in the aisle to be nearly isothermal, entropy generation in the airflow was very low compared to perimeter cooled scenarios.

ACKNOWLEDGMENT

This material is based upon work supported by the National Science Foundation Center for Energy Smart Electronic Systems (ES2) under Grant No. IIP-1134810. Any opinions, findings, and conclusions or recommendations expressed in this material are those of the author(s) and do not necessarily reflect the views of the National Science Foundation.

NOMENCLATURE

Be	Bejan number
N_S	entropy generation number
$\dot{m}$	mass flow rate (kg/s)
$\dot{Q}$	heat flux (W)
$\dot{S}_{gen}$	entropy generation (W/K)
T	absolute temperature (K)

Greek symbols

ϕ	irreversibility distribution ratio
η	overhead cooling efficiency
ξ	effectiveness

Subscripts

a	related to air
C	heat conduction
D	viscous dissipation
HX	related to heat exchanger
s	related to server
w	related to HX cooling fluid (water)
wl	related to HX wall

Superscripts

$'''$	per unit volume
*	characteristic scale

REFERENCES

[1] Heydari, A., and Sabounchi, P., 2004. "Refrigeration assisted spot cooling of a high heat density data center". In Thermal and Thermomechanical Phenomena in Electronic Systems, 2004. ITHERM'04., IEEE, pp. 601–606.

[2] Heydari, A., 2007. "Thermodynamics energy efficiency analysis and thermal modeling of data center cooling using open and closed-loop cooling systems". In ASME 2007 InterPACK Conference collocated with the ASME/JSME 2007 Thermal Engineering Heat Transfer Summer Conference, American Society of Mechanical Engineers, pp. 859–870.

[3] Wu, K., 2008. "A comparative study of various high density data center cooling technologies". PhD thesis, Stony Brook University.

[4] Kock, F., and Herwig, H., 2004. "Local entropy production in turbulent shear flows: a high-reynolds number model with wall functions". *International journal of heat and mass transfer,* ***47***(10), pp. 2205–2215.

[5] Ko, T., 2006. "Numerical investigation on laminar forced convection and entropy generation in a curved rectangular duct with longitudinal ribs mounted on heated wall". *International journal of thermal sciences,* ***45***(4), pp. 390–404.

[6] Herwig, H., and Kock, F., 2007. "Direct and indirect methods of calculating entropy generation rates in turbulent convective heat transfer problems". *Heat and mass transfer,* ***43***(3), pp. 207–215.

[7] Herwig, H., 2012. "The role of entropy generation in momentum and heat transfer". *Transactions of the ASME-C-Journal of Heat Transfer,* ***134***(3), p. 031003.

[8] Silva-Llanca, L., Ortega, A., Fouladi, K., del Valle, M., and Sundaralingam, V., 2015. "Entropy generation (exergy destruction) in CFD modeling for a legacy air-cooled data center". *(in preparation)*.

[9] Erden, H. S., Khalifa, H. E., and Schmidt, R. R., 2013. "Transient thermal response of servers through air temperature measurements". In ASME 2013 International Technical Conference and Exhibition on Packaging and Integration of Electronic and Photonic Microsystems, American Society of Mechanical Engineers, pp. 1–6.

[10] Demetriou, D. W., Erden, H. S., Khalifa, H. E., and Schmidt, R. R., 2014. "Development of an IT equipment lumped capacitance parameter database for transient data center simulations". In Thermal and Thermomechanical Phenomena in Electronic Systems (ITherm), 2014 IEEE Intersociety Conference on, IEEE, pp. 1330–1337.

[11] del Valle, M., and Ortega, A., 2014. "Numerical and compact models to predict the transient behavior of cross-flow heat exchangers in data center applications". In Thermal and Thermomechanical Phenomena in Electronic Systems (ITherm), 2014 IEEE Intersociety Conference on, IEEE, pp. 698–705.

[12] Shah, R. K., and Sekulic, D. P., 2003. *Fundamentals of heat exchanger design*. John Wiley & Sons.

[13] Spiga, M., and Spiga, G., 1988. "Transient temperature fields in crossflow heat exchangers with finite wall capacitance". *Journal of heat transfer,* ***110***(1), pp. 49–53.

[14] Bejan, A., 1996. *Entropy generation minimization: the method of thermodynamic optimization of finite-size systems and finite-time processes*, Vol. 2. CRC press.

[15] Shah, A. J., Carey, V. P., Bash, C. E., and Patel, C. D., 2008. "Exergy analysis of data center thermal management systems". *Journal of Heat Transfer,* ***130***(2), p. 021401.